Supporting information

Near-infrared II photochromic behavior triggered by green light in an *in situ* protonated dithienylethene functionalized by quinoxalinone moieties

Ziyong Li*, Jinzhao Song, Qilian Wang, Yongliang Feng, Qingxin Song, Sixin Wang, Qianqian Nie, Fan He, Haining Zhang, Hui Guo*

Luoyang Key Laboratory of Organic Functional Molecules, College of Food and Drug, College of Chemistry and Chemical Engineering, Luoyang Normal University, Luoyang 471934, P. R. China

Corresponding authors E-mail: liziyong@mails.ccnu.edu.cn (Z. Li); guohui@lynu.edu.cn (H. Guo)

1. General information

1.1 Materials

All manipulations were carried out under a nitrogen atmosphere by using standard Schlenk techniques unless otherwise stated. THF was distilled under nitrogen from sodium-benzophenone. DMF was dried by $MgSO_4$ and distilled under reduced pressure. The intermediates **1**[1] and **2**[2,3] were prepared by reported literature method, respectively. All other starting materials were obtained commercially as analytical-grade from Energy Chemical Reagent Co., Ltd (Shanghai, China) and used without further purification.

1.2 Instruments

^1H and ^{13}C NMR spectra were collected on German BRUKER AVANCE III 400 MHz (all the chemical shifts are relative to TMS). High resolution mass spectra were obtained on SCIEX X-500R QTOF (ESI mode). All the absorption spectra were collected on a SHIMADZU UV-2600 UV-Vis spectrophotometer, and the fluorescence spectra were obtained on a Hitachi F-7000 fluorescent spectrophotometer. In the photochromic experiments, the visible light irradiation experiments were carried out by using 30 W Blue lamp (460-470 nm) and 30 W Green lamp (520-530 nm), and the NIR light irradiation experiments were carried out by using 30 W Near infrared lamp (730-740 nm) and 30 W Near infrared lamp (1000-1050 nm), respectively. All these LED lamps were purchased from Shenzhen Boya Technology Co., Ltd (China).

1.3 Determination of the cyclization and cycloreversion quantum yields

The cyclization and cycloreversion quantum yields of **QDTE** and **QDTE-2H** were determined according to the standard procedure reported in previous literatures.[4,5] For the cyclization quantum yields, potassium ferrioxalate ($K_3[Fe(C_2O_4)_3]$) was used as actinometer.[6] The light intensity of blue or green light was determined by following steps: i) 3.0 mL of 0.006 M $K_3[Fe(C_2O_4)_3]$ solution in 0.05 M H_2SO_4 was irradiated for 180 s; ii) 0.5 mL phenanthroline (0.1 wt % in 0.5 M H_2SO_4 /1.6 M NaOAc) were added subsequently; iii) measuring the absorbance at 510 nm before and after irradiation. The light intensity could be calculated via Eq. (1).

$$I_0 = \frac{\Delta A_{510nm}}{\Delta t * \varepsilon_{510nm} * \emptyset_{irr} * 1000} * \frac{3.5mL}{3.0mL} \qquad (1)$$

In which ΔA_{510nm} is the difference of the absorption at 510 nm for an irradiated versus a nonirradiated solution, Δt is the irradiation time, ε_{510nm} is 11100 M^{-1} cm^{-1} and Φ_{irr} is the quantum yield at the irradiation

wavelength (1.10 for 460 nm; 0.65 for 520 nm).

Because the wavelength of the irradiation light that was needed for the ring-opening was out of the range for ferrioxalate actinometry (220-550 nm). Therefore, for the cycloreversion quantum yields of **QDTE** and **QDTE-2H**, aberchrome 670 was used as actinometer.[6] The light intensity at 600 nm was determined by following steps: i) 3.0 mL aberchrome 670 solution (1.0×10^{-4} M in toluene) was irradiated with 365 nm light; ii) the formed isomer was irradiated back with 600 nm light, iii) measuring the absorbance at 519 nm before and after irradiation. The light intensity at 600 nm could be calculated via Eq. (2).

$$I_0 = \frac{\Delta A_{519nm}}{\Delta t * \varepsilon_{519nm} * \emptyset_{irr} * 1000 * (1 - 10^{-A'})} \qquad (2)$$

In which ΔA_{519nm} is the difference of the absorption at 519 nm before and after irradiation, Δt is the irradiation time, ε_{519nm} is 7760 M^{-1} cm^{-1}, Φ_{irr} is the quantum yield at the irradiation wavelength (0.27 for 600 nm), $1\text{-}10^{-A'}$ is the percentage of absorbance photons by the solution at irradiation wavelength, and A' is the initial absorbance at the irradiation wavelength.

Then, the solutions of ring-open isomers **QDTE(o)** and **QDTE-2H(o)** (3.0 mL, 2.0×10^{-5} M) were irradiated with the same investigated light source, and the changes at corresponding maximum absorption wavelength were measured immediately. The cyclization quantum yields could be calculated via Eq. (3). Moreover, the similar operations were performed on ring-closed isomers, and the cycloreversion quantum yields could also be calculated via Eq. (3).

$$\emptyset = \frac{\Delta A / \Delta t}{(1 - 10^{-A'}) * \varepsilon * I_0 * 1000} \qquad (3)$$

In which $\Delta A/\Delta t$ is the change rate of absorbance upon irradiating at excitation wavelength, $1\text{-}10^{-A'}$ is the percentage of absorbance photons by the solution at irradiation wavelength, ε is extinction coefficient at detection wavelength, and I_0 is the light intensity calculated above.

1.4 Determination of the fluorescence quantum yields

The fluorescence quantum yields (Φ_f) of **QDTE** and **QDTE-2H** in the various solvents were approximatively determined according to the following equation:

$$\emptyset_s = \emptyset_{ref} \times \frac{F_s}{F_{ref}} \times \frac{A_{ref}}{A_s} \times \frac{n_s^2}{n_{ref}^2}$$

in which Φ_{ref} is the fluorescence quantum yield of reference, F is the area under the emission spectra, A is the absorbance at the excitation wavelength, n is the refractive index of solvent. s and ref stand for sample and reference, respectively. We chose quinoline sulfate (Φ_{ref} = 0.55, in 0.1 M aqueous H_2SO_4) as the reference. Absorbance of the unknown samples and the standard should be similar and small.[7]

1.5 Theoretical calculation

Theoretical calculation was carried out using the Gaussian 09 software. Geometry optimization was performed using density functional theory (DFT) at B3LYP/6-31G* level of theory. The electronic distribution of the frontier molecular orbitals was drawn using Gaussview 5.0.

2. Experimental section

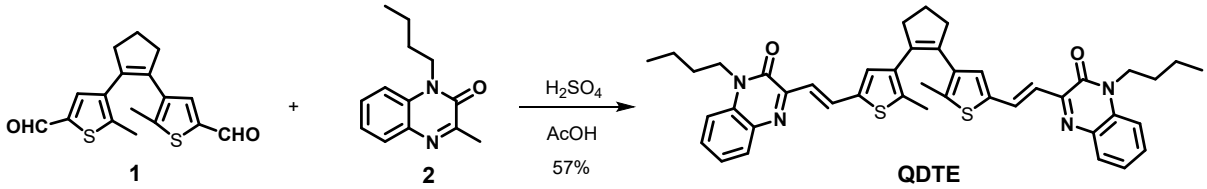

Scheme S1. Synthetic route of quinoxalinone-functionalized DTE derivative (**QDTE**).

To a solution of **1** (316 mg, 1.0 mmol) and **2** (476 mg, 2.2 mmol) in acetic acid (10 mL) was added catalytic concentrated sulfuric acid under nitrogen. The reaction mixture was stirred at 50 °C for 16 h in the dark. The reaction mixture was cooled and poured into 100 mL of water. Then the resulting solution was neutralized with 2.0 mol/L Na_2CO_3 aqueous solution and extracted with ethyl acetate (3 × 20 mL). The combined organic layer was dried with anhydrous Na_2SO_4, filtered and concentrated under vacuum. Then the crude product was purified by column chromatography (petroleum ether/ethyl acetate = 9:1) to give target **QDTE** as a yellow solid (406 mg, yield: 57%). ^{1}H NMR (400 MHz, $CDCl_3$) δ 8.16 (d, J = 15.8 Hz, 2H), 7.83 (d, J = 7.4 Hz, 2H), 7.48 (t, J = 7.4 Hz, 2H), 7.39 – 7.27 (m, 6H), 7.02 (s, 2H), 4.35 – 4.20 (m, 4H), 2.80 (t, J = 7.4 Hz, 4H), 2.18 – 2.01 (m, 2H), 1.96 (s, 6H), 1.82 – 1.71 (m, 4H), 1.50 (m, 4H), 1.01 (t, J = 7.4 Hz, 6H). ^{13}C NMR (100 MHz, $CDCl_3$) δ 154.69, 152.27, 138.40, 137.90, 136.72, 134.47, 133.83, 131.90, 131.39, 131.12, 129.89, 129.29, 123.61, 120.61, 113.58, 42.20, 38.51, 29.30, 22.85, 20.33, 14.88, 13.82. HRMS (ESI-TOF) m/z: $[M + H]^+$ calcd for $C_{43}H_{45}N_4O_2S_2$ 713.2984; found 713.2995.

3. Supporting Figures

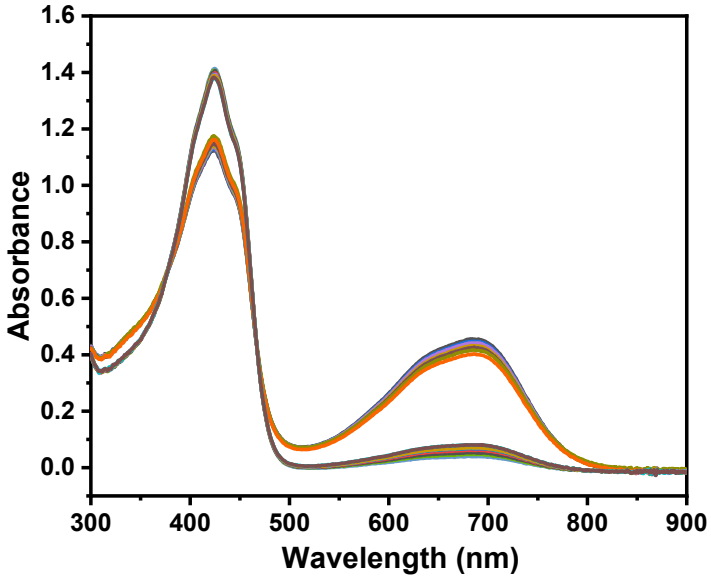

Figure S1. The absorption spectra changes of **QDTE** in DMSO (2.0×10^{-5} mol/L) upon alternating irradiation with blue light at 460-470 nm and NIR I light at 730-740 nm for ten times.

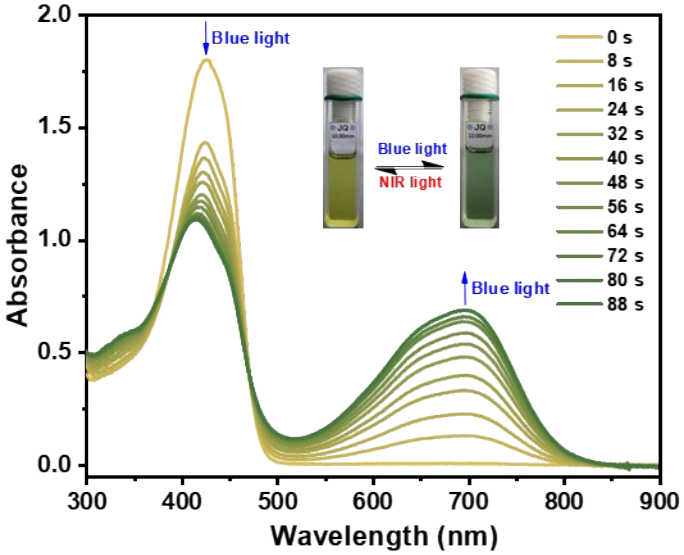

Figure S2. The absorption spectra changes of **QDTE** in $CHCl_3$ (2.0×10^{-5} mol/L) upon irradiation with blue light at 460-470 nm. The insets show the corresponding color changes upon photoirradiation.

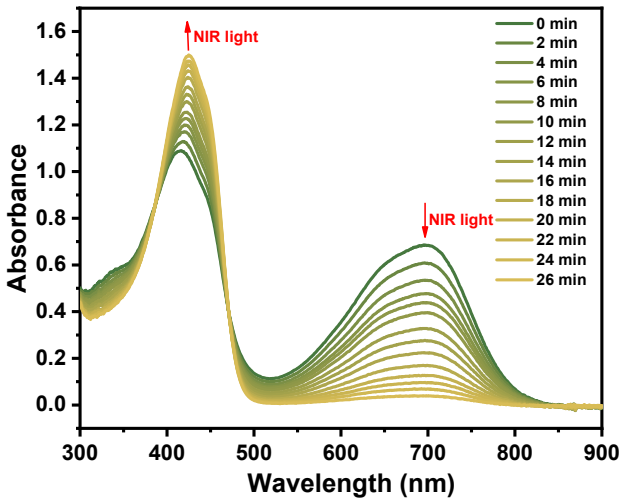

Figure S3. The absorption spectra changes of **QDTE** in $CHCl_3$ (2.0×10^{-5} mol/L) upon irradiation with NIR I light at 730-740 nm.

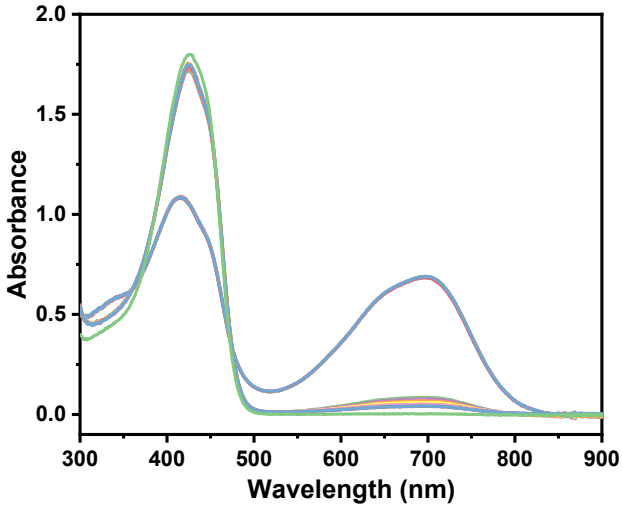

Figure S4. The absorption spectra changes of **QDTE** in $CHCl_3$ (2.0×10^{-5} mol/L) upon alternating irradiation with blue light at 460-470 nm and NIR light at 730-740 nm for ten times.

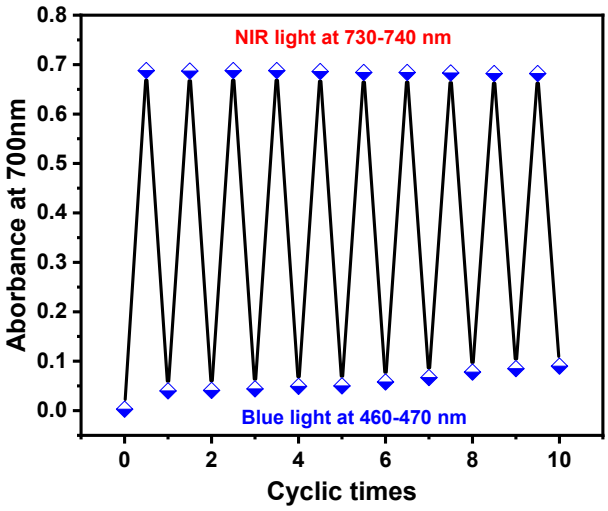

Figure S5. The absorption spectra changes of **QDTE** in $CHCl_3$ (2.0×10^{-5} mol/L) upon alternating irradiation with blue light at 460-470 nm and NIR I light at 730-740 nm for ten times.

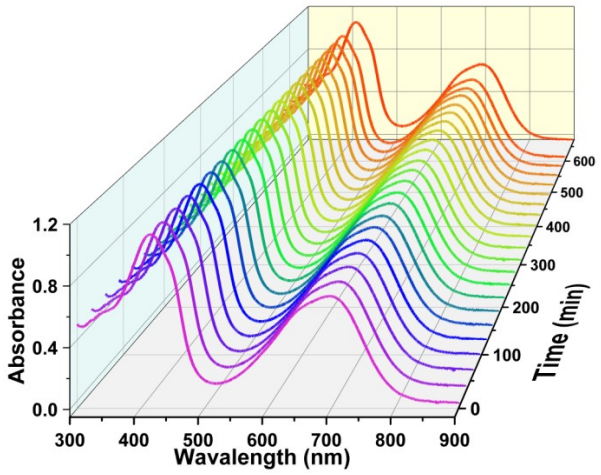

Figure S6. The thermal stability of the closed isomer **QDTE(c)** in $CHCl_3$ at 40 °C by monitoring changes in λ_{max} of **QDTE(c)** at PSS.

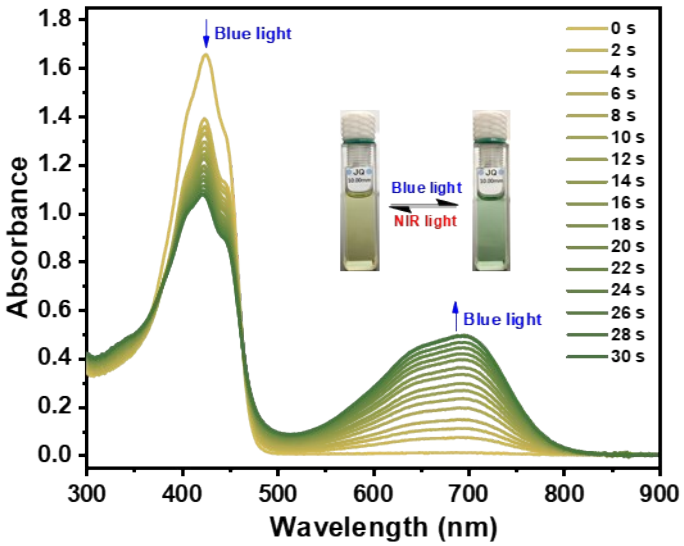

Figure S7. The absorption spectra changes of **QDTE** in toluene (2.0×10^{-5} mol/L) upon irradiation with blue light at 460-470 nm. The insets show the corresponding color changes upon photoirradiation.

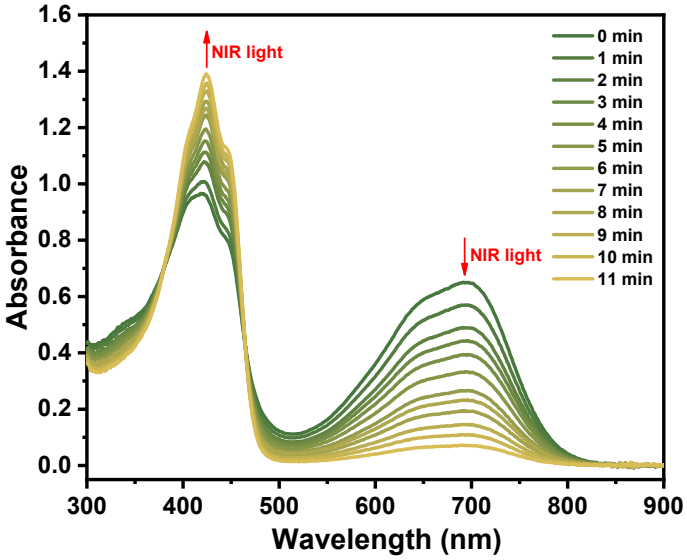

Figure S8. The absorption spectra changes of **QDTE** in toluene (2.0×10^{-5} mol/L) upon irradiation with NIR I light at 730-740 nm.

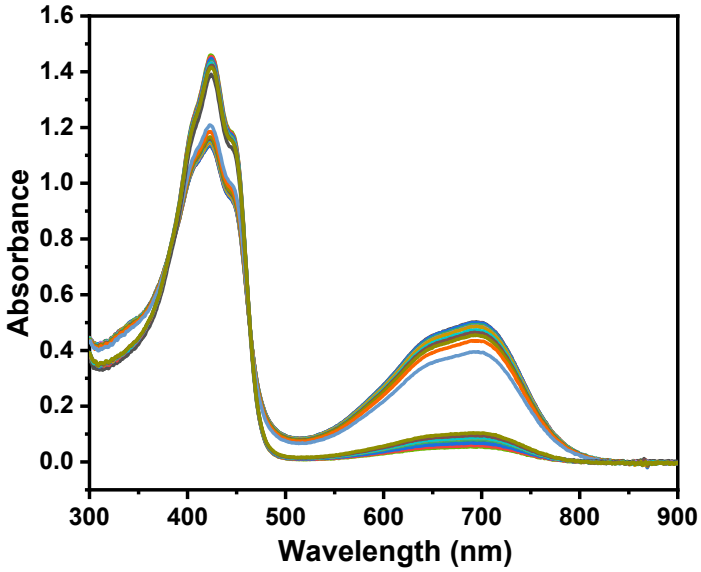

Figure S9. The absorption spectra changes of **QDTE** in toluene (2.0×10^{-5} mol/L) upon alternating irradiation with blue light at 460-470 nm and NIR I light at 730-740 nm for ten times.

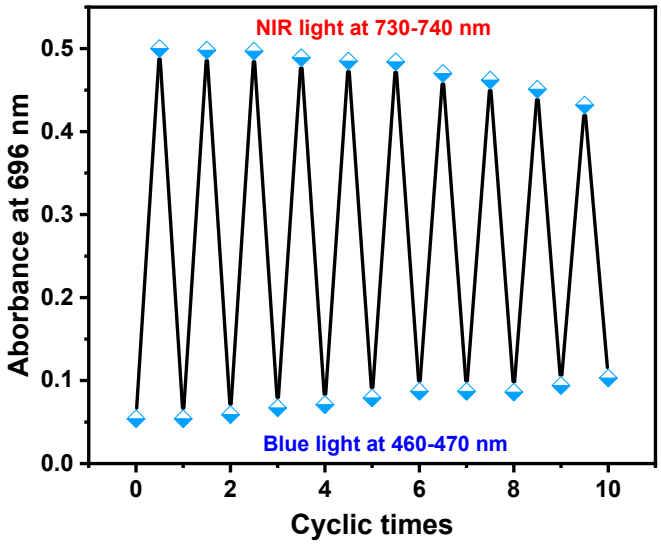

Figure S10. The absorption spectra changes of **QDTE** in toluene (2.0×10^{-5} mol/L) upon alternating irradiation with blue light at 460-470 nm and NIR I light at 730-740 nm for ten times.

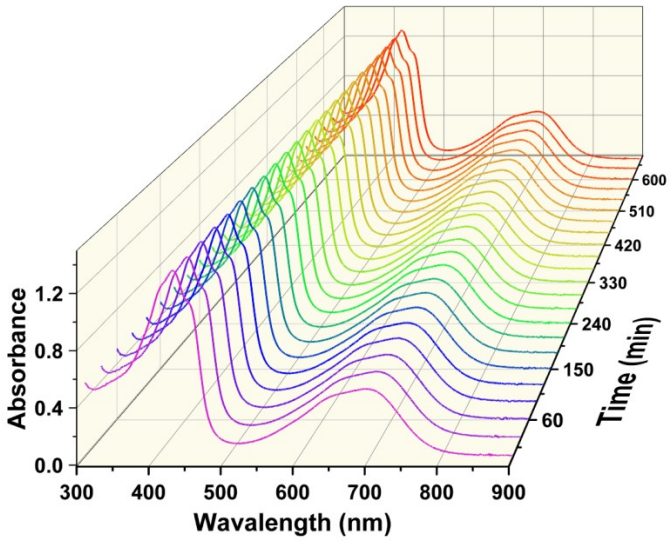

Figure S11. The thermal stability of the closed isomer **QDTE(c)** in toluene at 40 ℃ by monitoring changes in λ_{max} of **QDTE(c)** at PSS.

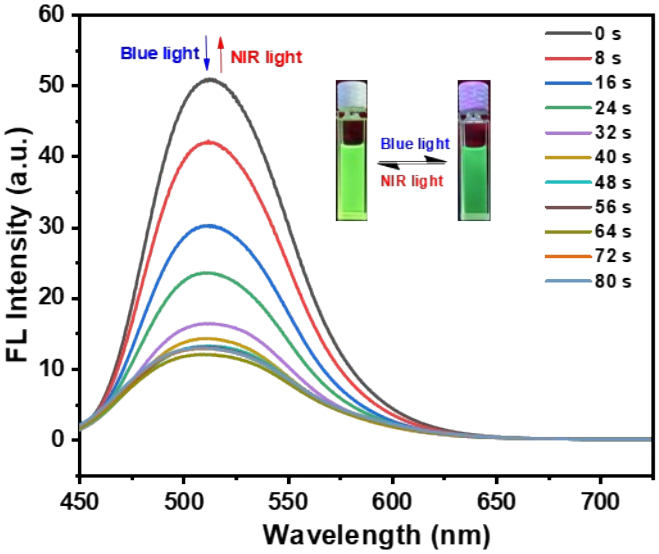

Figure S12. The fluorescence spectra changes of **QDTE** in $CHCl_3$ (2.0×10^{-5} mol/L) upon alternating irradiation with blue light at 460-470 nm light and NIR I light at 730-740 nm (a). (Inset) Corresponding fluorescent color changes upon photoirradiation (λ_{ex} = 440 nm).

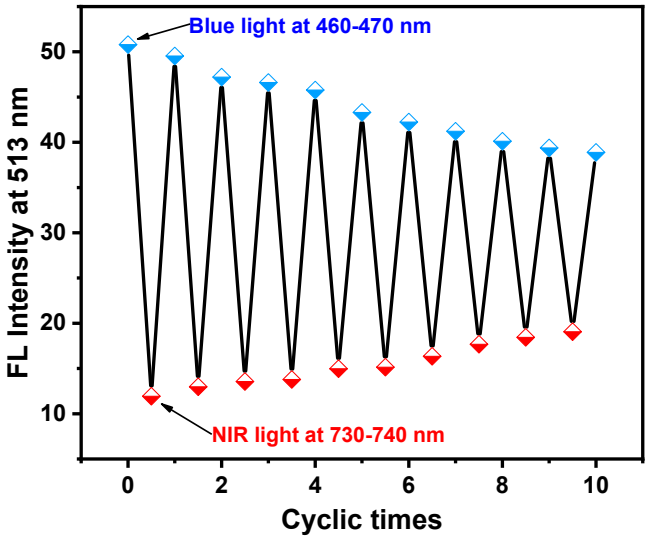

Figure S13. The fluorescence fatigue resistance of **QDTE** in $CHCl_3$ (2.0×10^{-5} mol/L) for ten cycles.

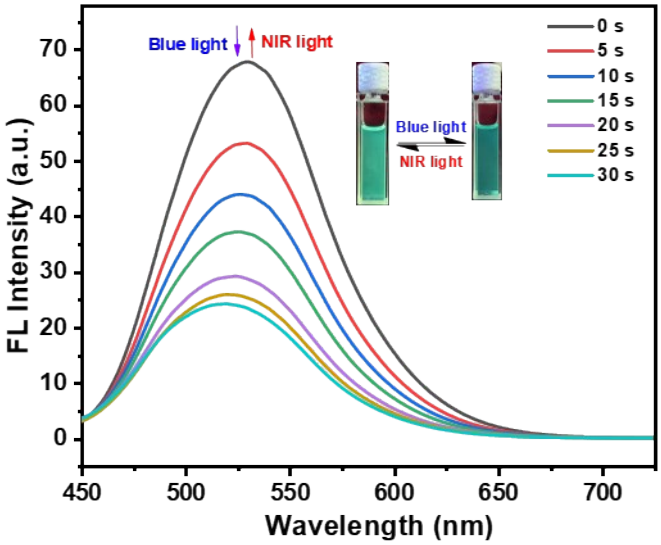

Figure S14. The fluorescence spectra changes of **QDTE** in toluene (2.0×10^{-5} mol/L) upon alternating irradiation with blue light at 460-470 nm light and NIR I light at 730-740 nm (a). (Inset) Corresponding fluorescent color changes upon photoirradiation (λ_{ex} = 440 nm).

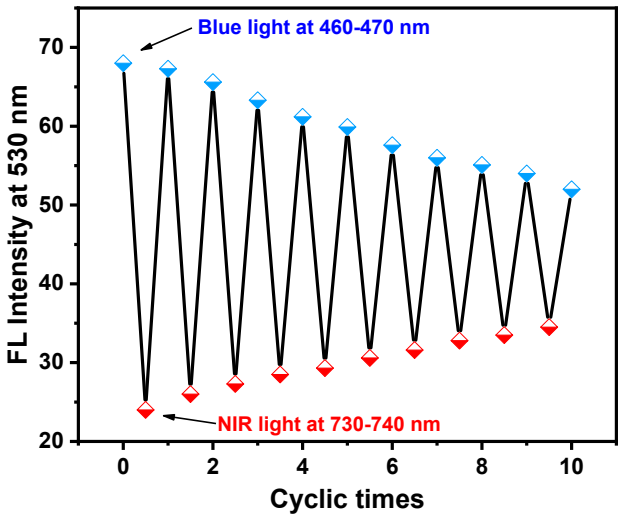

Figure S15. The fluorescence fatigue resistance of **QDTE** in toluene (2.0×10^{-5} mol/L) for ten cycles.

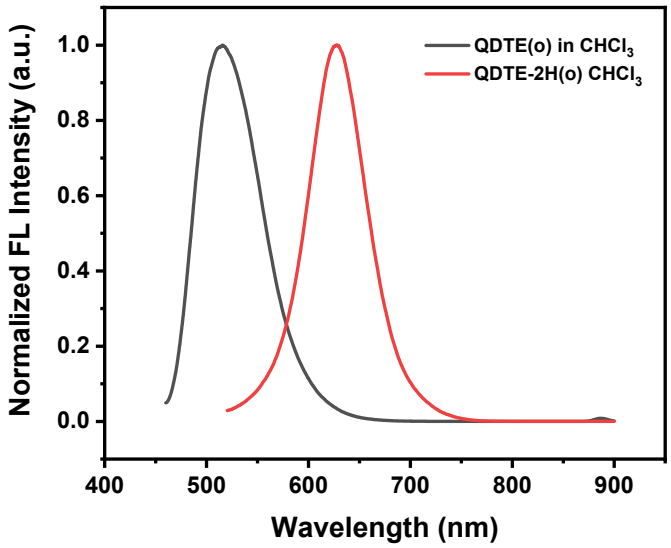

Figure S16. The normalized fluorescence spectra of the open isomer **QDTE(o)** and **QDTE-2H(o)** in $CHCl_3$ (2.0×10^{-5} mol/L) (λ_{ex} = 440 nm, 500 nm, respectively).

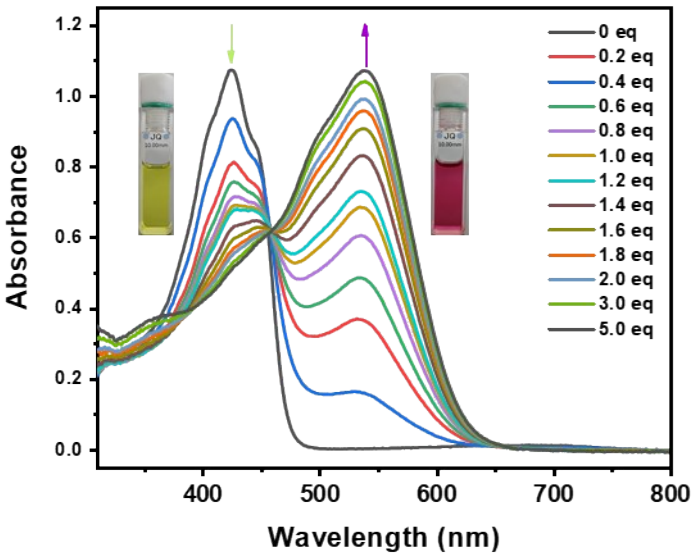

Figure S17. The absorption spectra changes of the open isomer **QDTE(o)** in the presence of TFA (0-5.0 eq.) in toluene (2.0×10^{-5} mol/L). The insets show the corresponding color changes before and after addition of 5.0 eq. TFA.

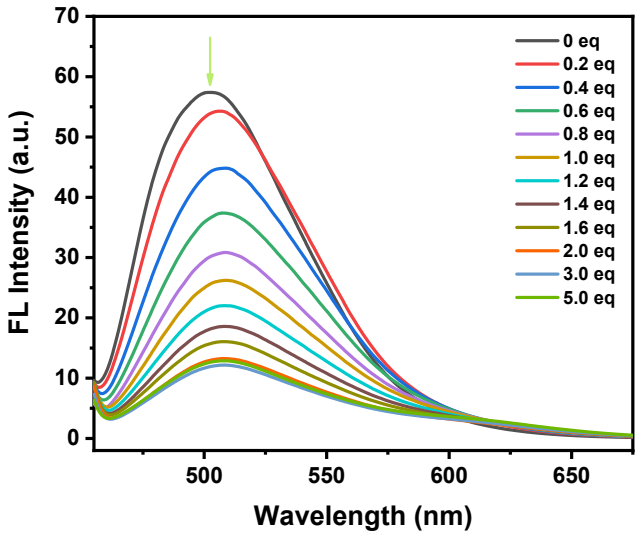

Figure S18. The fluorescence spectra changes of the open isomer **QDTE(o)** in the presence of TFA (0-5.0 eq.) in toluene (2.0×10^{-5} mol/L) (λ_{ex} = 440 nm).

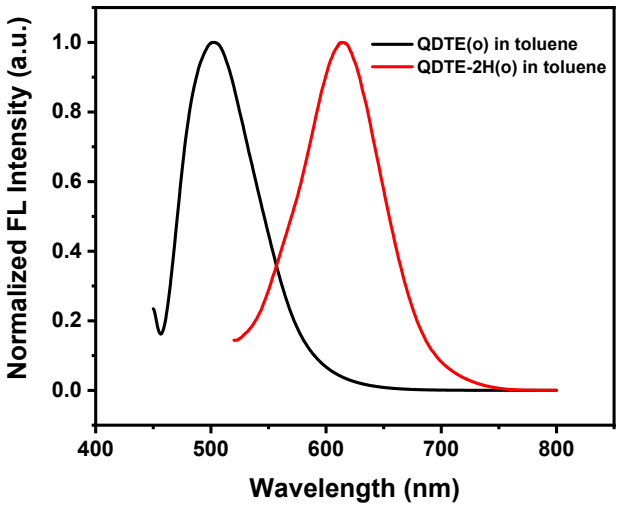

Figure S19. The normalized fluorescence spectra of the open isomer **QDTE(o)** and **QDTE-2H(o)** in toluene (2.0×10^{-5} mol/L) (λ_{ex} = 440 nm, 500 nm, respectively).

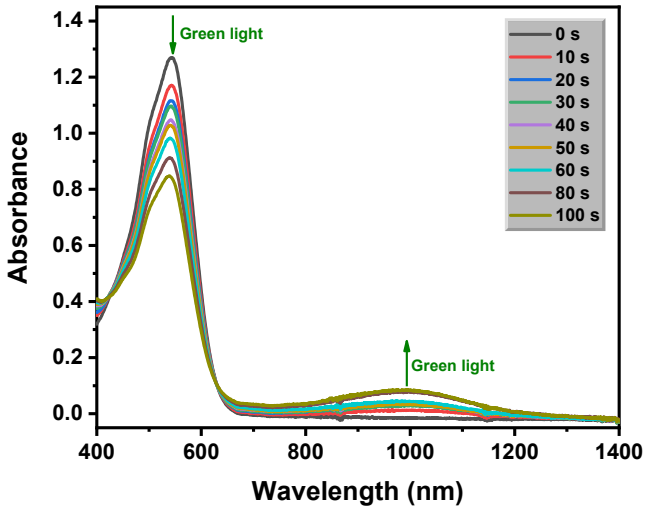

Figure S20. The absorption spectra changes of as-protonated **QDTE-2H** in toluene (2.0×10^{-5} mol/L) upon irradiation with green light at 520-530 nm.

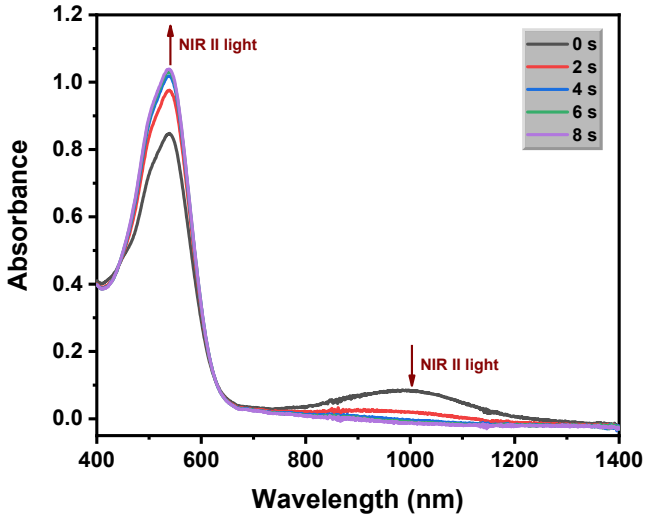

Figure S21. The absorption spectra changes of as-protonated **QDTE-2H** in toluene (2.0×10^{-5} mol/L) upon irradiation with NIR II light at 1000-1050 nm.

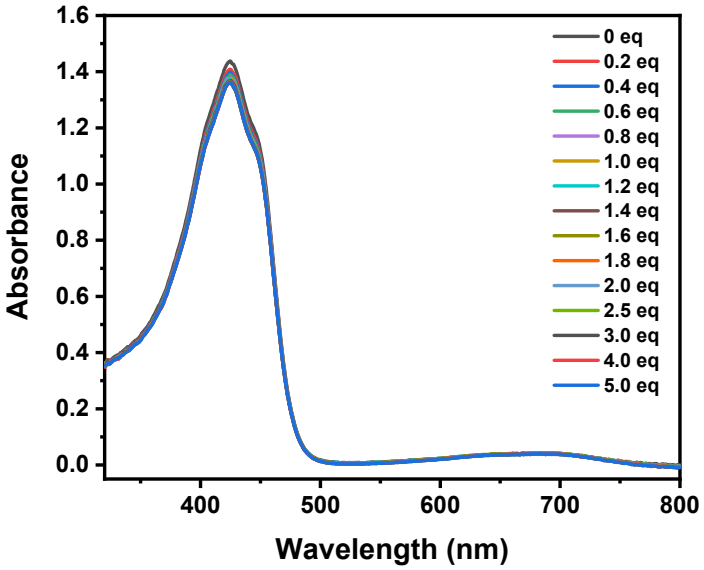

Figure S22. The absorption spectra changes of the open isomer **QDTE(o)** in the presence of TFA (0-5.0 eq.) in DMSO (2.0×10^{-5} mol/L).

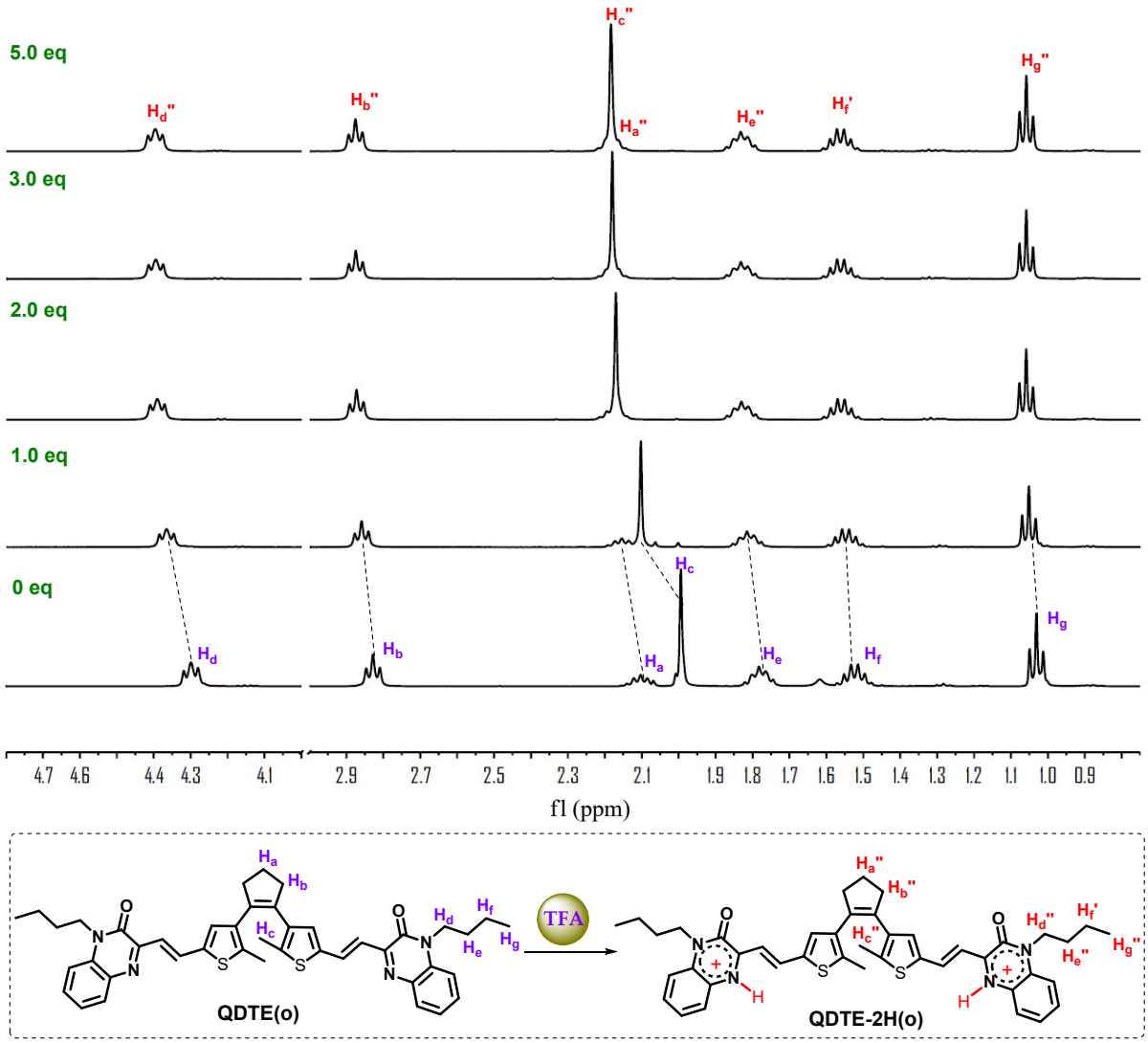

Figure S23. The partial ^{1}H NMR spectral changes of the open isomer **QDTE(o)** in the presence of TFA-D1 (0-5.0 eq.) in $CDCl_3$ at room temperature.

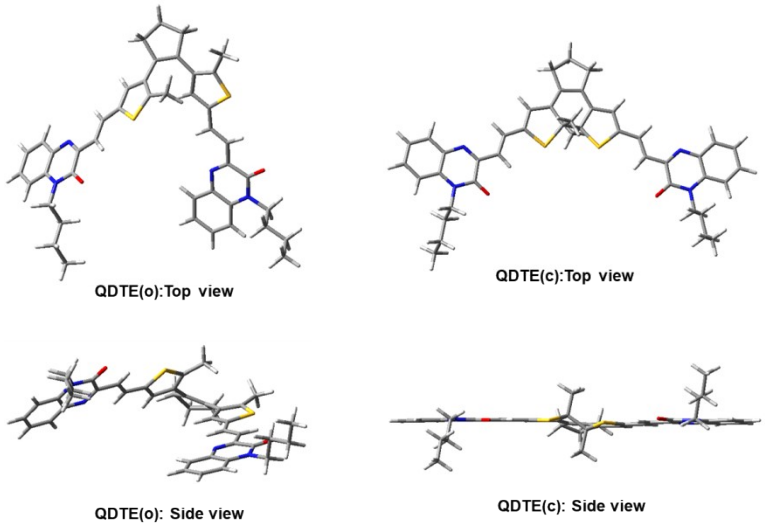

Figure S24. The corresponding energy-minimized structures of **QDTE(o)** and **QDTE(c)** based on DFT calculations at the B3LYP/6-31G* level using the Gaussian 09 program.

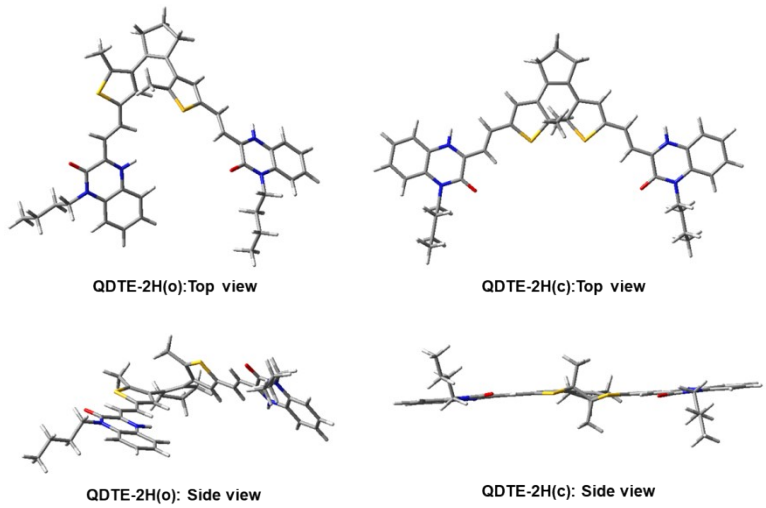

Figure S25. The corresponding energy-minimized structures of **QDTE-2H(o)** and **QDTE-2H(c)** based on DFT calculations at the B3LYP/6-31G* level using the Gaussian 09 program.

4. NMR and Mass spectra

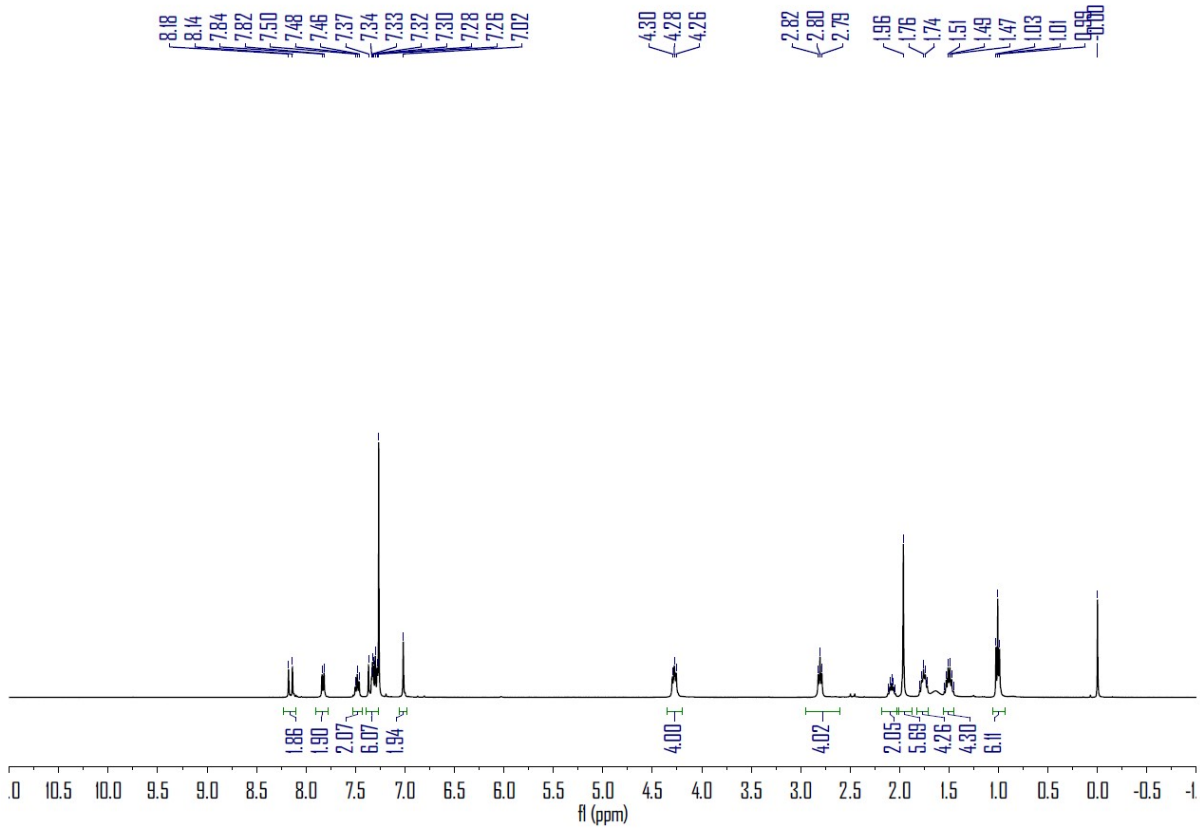

Figure S26. 400 MHz ^{1}H NMR spectrum of **QDTE** in $CDCl_3$ at room temperature.

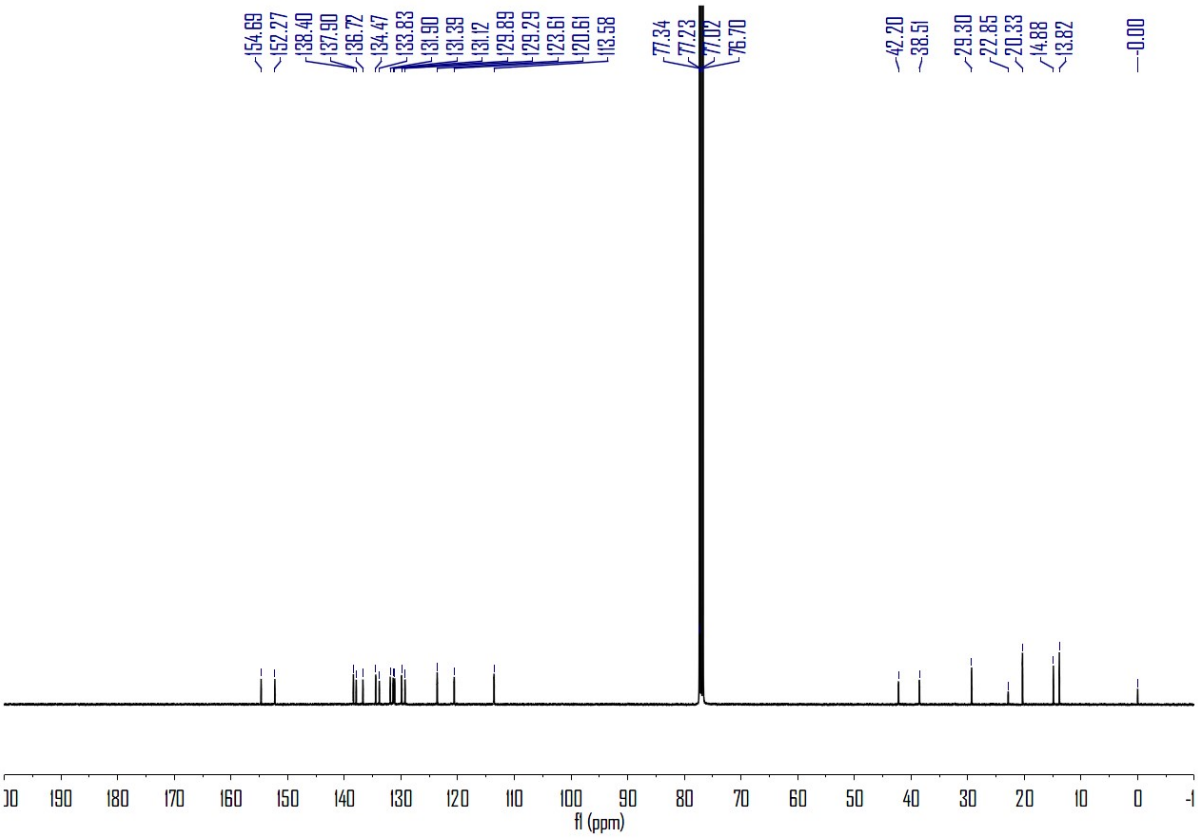

Figure S27. 100 MHz ^{13}C NMR spectrum of **QDTE** in $CDCl_3$ at room temperature.

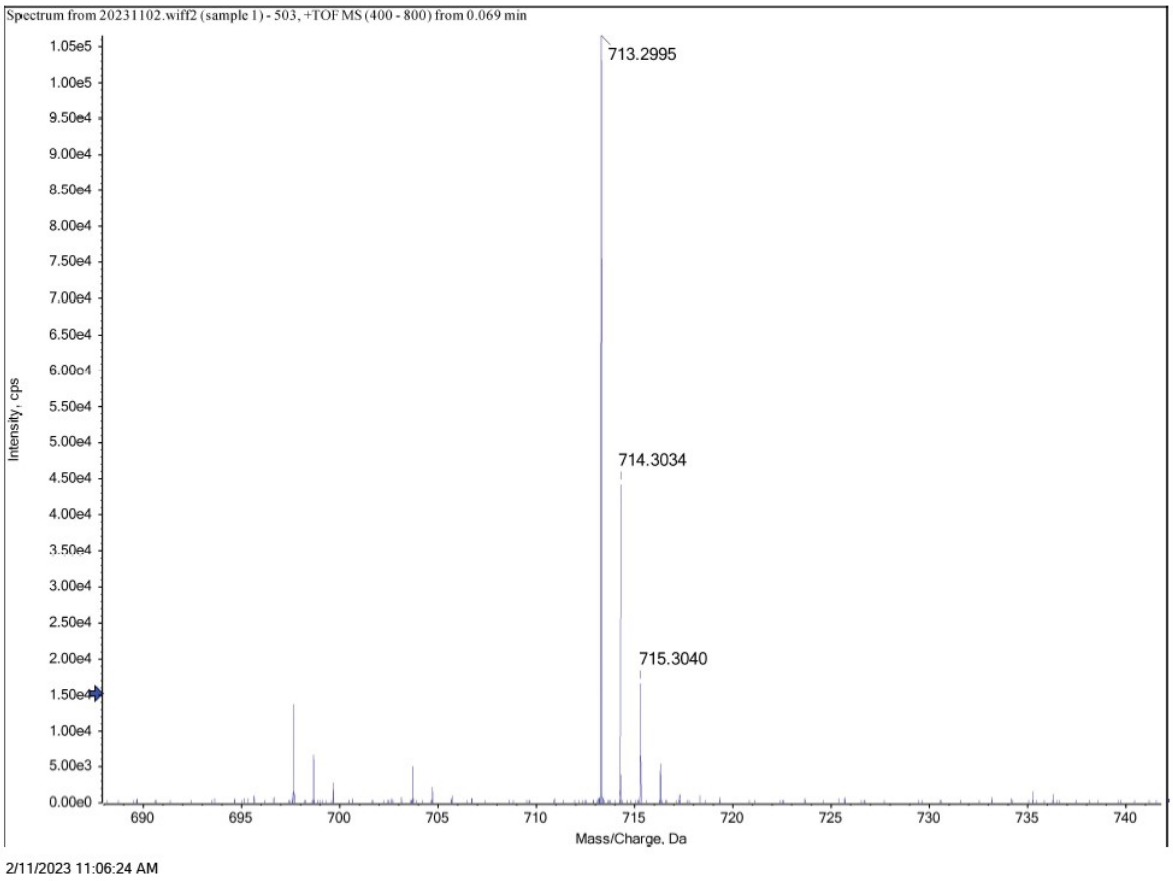

Figure S28. HRMS of **QDTE**.

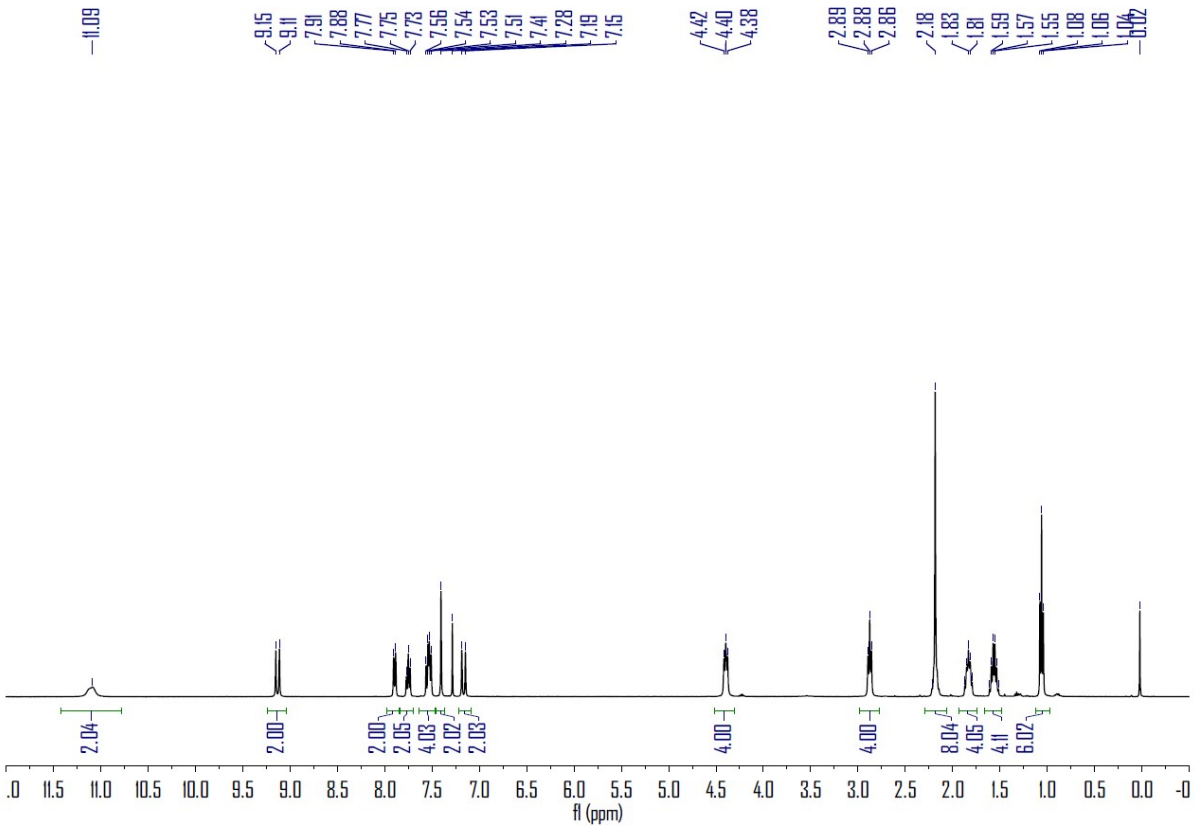

Figure S29. 400 MHz ^{1}H NMR spectrum of **QDTE(o) in the presence of TFA-D1 (5.0 eq.)** in $CDCl_3$ at room temperature.

5. References

1 L. N. Lucas, J. J. D. Jong, J. H. Esch, R. M. Kellogg and B. L. Feringa, Syntheses of dithienylcyclopentene optical molecular switches, *Eur. J. Org. Chem.*, 2003, **2003**, 155-166.

2 P. Zhang, H. Kuang, Y. Xu, L. Shi, W. Cao, K. Zhu, L. Xu and J. Ma, Rational design of a high-performance quinoxalinone-based AIE photosensitizer for image-guided photodynamic therapy, *ACS Appl. Mater. Interfaces*, 2020, **12**, 42551-42557.

3 P. Ghosh, N. Y. Kwon, S. Kim, S. Han, S. H. Lee, W. An, N. K. Mishra, S. B. Han and I. S. Kim, C-H methylation of iminoamido heterocycles with sulfur ylides, *Angew. Chem. Int. Ed.,* 2021, **60**, 191-196.

4 S. Fredrich, R. Göstl, M. Herder, L. Grubert and S. Hecht, Switching diarylethenes reliably in both directions with visible light, *Angew. Chem. Int. Ed.,* 2016, **55**, 1208-1212.

5 H. Xi, Z. Zhang, W. Zhang, M. Li, C. Lian, Q. Luo, H. Tian and W. -H. Zhu, All-visible light-Activated dithienylethenes induced by intramolecular proton transfer, *J. Am. Chem. Soc.,* 2019, **141**, 18467-18474.

6 M. Montalti, A. Credi, L. Prodi, M. T. Gandolfi, Handbook of Photochemistry, 3rd ed.; CRC Press: Boca Raton, 2006.

7 A. P. Glaze, H. G. Heller and J. Whittall, Photochromic heterocyclic fulgides. Part 7. (E)-Adamantylidene-[1-(2,5-dimethyl-3-furyl)ethylidene]succinic anhydride and derivatives: model photochromic compounds for optical recording media, *J. Chem. Soc. Perk. Trans.,* 1992, **2**, 591-594.